HHS Public Access

Author manuscript

Traffic. Author manuscript; available in PMC 2017 April 01.

Published in final edited form as:

Traffic. 2016 April ; 17(4): 400–415. doi:10.1111/tra.12375.

Molecular basis for the interaction between Adaptor Protein Complex 4 (AP4) β4 and its accessory protein, tepsin

Meredith N. Frazier[1,2], **Alexandra K. Davies**[3], **Markus Voehler**[2,4], **Amy K. Kendall**[1,2], **Georg H. H. Borner**[5], **Walter J. Chazin**[2,4], **Margaret S. Robinson**[3], and **Lauren P. Jackson**[1,2]

[1]Department of Biological Sciences, Vanderbilt University, Nashville, TN, USA

[2]Center for Structural Biology, Vanderbilt University, Nashville, TN, USA

[3]Cambridge Institute for Medical Research, Department of Clinical Biochemistry, University of Cambridge, Hills Road, Cambridge, United Kingdom

[4]Department of Biochemistry and Chemistry, Vanderbilt University, Nashville, TN, USA

[5]Max Planck Institute of Biochemistry, Department of Proteomics and Signal Transduction, Martinsried, Germany

Abstract

The adaptor protein 4 (AP4) complex (ε/β4/μ4/σ4 subunits) forms a non-clathrin coat on vesicles departing the *trans*-Golgi network (TGN). AP4 biology remains poorly understood, in stark contrast to the wealth of molecular data available for the related clathrin adaptors AP1 and AP2. AP4 is important for human health because mutations in any AP4 subunit cause severe neurological problems, including intellectual disability and progressive spastic para- or tetraplegia. We have used a range of structural, biochemical, and biophysical approaches to determine the molecular basis for how the AP4 β4 C-terminal appendage domain interacts with tepsin, the only known AP4 accessory protein. We show that tepsin harbors a hydrophobic sequence, LFxG[M/L]x[L/V], in its unstructured C-terminus, which binds directly and specifically to the C-terminal β4 appendage domain. Using NMR chemical shift mapping, we define the binding site on β4 appendage by identifying residues on the surface whose signals are perturbed upon titration with tepsin. Point mutations in either the tepsin LFxG[M/L]x[L/V] sequence or in its cognate binding site on β4 abolish binding *in vitro*. In cells, the same point mutations greatly reduce the amount of tepsin that interacts with AP4. However, they do not abolish the binding between tepsin and AP4 completely, suggesting the existence of additional interaction sites between AP4 and tepsin. These data provide one of the first detailed mechanistic glimpses at AP4 coat assembly and should provide an entry point for probing the role of AP4 coated vesicles in cell biology, and especially in neuronal function.

Correspondence to lauren.p.jackson@vanderbilt.edu.

The authors declare no conflicts of interest.

Keywords

membrane trafficking; vesicle coats; non-clathrin coats; adaptor protein complexes; biochemistry; structural biology; cell biology

Introduction

Large coat protein complexes play central roles in many membrane trafficking pathways by driving vesicle coat formation at specific organelle membranes. The mammalian AP (Assembly Polypeptide) adaptor protein complexes (APs 1–5, COPI F-subcomplex) are a family of heterotetrameric complexes that recognize membrane components, transmembrane protein cargo, and additional machinery required for vesicle coat assembly. While the clathrin adaptors AP1 and AP2 are well-characterized mechanistically and functionally [1–15], the molecular structures and cellular functions of non-clathrin adaptors like AP4 and AP5 remain poorly understood. The AP4 complex (ε/β4/μ4/σ4 subunits) (Figure 1A) is recruited to the *trans*-Golgi network (TGN) by the small GTPase, Arf1, in its GTP-bound state [16]. AP4 has been implicated in polarized cargo sorting in both epithelial cells [17] and neurons [18,19], and the C-terminus of μ4 can bind a YKFFE motif found in amyloid precursor protein (APP) [20]. Although AP4 is ubiquitously expressed [21,22], the most striking phenotypes are associated with the brain. A β4 knockout mouse exhibits mis-sorting of LDL, AMPA, and δ2 glutamate receptors from somatodendrites to axons [19] but shows no further significant anatomical abnormalities. In contrast, human patients with mutations in any one of the four AP4 subunits [23–26] suffer from a severe “AP-4 deficiency syndrome” characterized by early onset of severe intellectual disability, growth retardation, stereotypic laughter, progressive spasticity and an inability to walk ([23], reviewed in [27]). AP4 thus likely plays a key role in neurological development and function, but the underlying mechanism remains unclear. It is therefore important to identify and understand the machinery required to form an AP4 coat, specifically the nature of the full complement of proteins in this coat, in order to uncover both the fundamental cellular function of AP4 and its role in human disease.

Unlike the AP1 and AP2 clathrin adaptors, an understanding of AP4 biology using traditional genetic and biochemical approaches has been hampered for two main reasons. During evolution, AP4 was lost in multiple eukaryotic lineages [28,29], including model organisms like yeast, worms, and flies. In addition, AP4 is much less abundant than either AP1 or AP2 [27]. This has made standard fractionation-based proteomic analysis of AP4 vesicles unfeasible. However, progress was made using a comparative proteomic profiling method in which coated vesicle fractions were prepared under different conditions [30]. Similar patterns of enrichment across different vesicle preps were used to predict association, and this led to the identification of tepsin as the first AP4 accessory protein. Full-length tepsin was shown to bind specifically to the β4 C-terminal appendage domain (residues 612–739) [30].

Tepsin (Figure 1A) is a member of the epsin family of mammalian post-Golgi trafficking proteins, which includes the plasma membrane epsins1–3 and TGN/endosomal epsinR. All

epsins contain an epsin N-terminal homology (ENTH) domain followed by mostly unstructured C-termini. Tepsin is distinct among family members in possessing a second folded structural domain, predicted to be most similar to a VHS domain ([30]). In clathrin coated vesicles (CCVs), epsins function as accessory proteins by binding phosphoinositides via their ENTH domains [31–33]; recognizing cargo via ubiquitin interacting motifs (UIMs) in epsins1–3 [34,35] or folded structural domains in epsinR [36]; weakly binding endocytic SNAREs [37]; and interacting with clathrin [38] [39] and either AP1 or AP2 via short linear amino acid motifs [2,38,40] or short stretches of secondary structure [41]. However, quantitative proteomics [30] suggest epsin1 is present at only very low levels in endocytic CCVs, while tepsin is a major component in AP4 vesicles. Tepsin lacks characterized motifs for binding ubiquitin, clathrin, and AP1 or AP2. Furthermore, tepsin requires AP4 for its membrane recruitment [30]; epsins1–3 are recruited to membranes directly through binding phosphoinositides [31].

Since tepsin is the first established AP4 accessory protein, we set out to identify and characterize the mechanism of the interaction between β4 and tepsin in order to obtain the first mechanistic information about AP4 coat formation. We show the β4 C-terminal appendage domain interacts specifically with a short, hydrophobic sequence in the unstructured tepsin C-terminus; this sequence is one of the first candidate AP4-specific binding motifs. The interaction is specific to the β4 C-terminus, because the tepsin motif cannot bind the β appendage domains of AP1 or AP2. Mutation of conserved residues in the tepsin motif abolishes binding to β4 *in vitro*. We use structural and biophysical methods combined with mutagenesis to identify and confirm key tepsin binding residues on the surface of the β4 appendage domain. Finally, we demonstrate the functional relevance of this interaction in cultured cells. Specific point mutations in either the β4 appendage domain or the tepsin motif greatly reduce the amount of tepsin bound to AP4 in HeLa cell lines. However, the mutations do not completely abolish the interaction between tepsin and AP4 and do not prevent the recruitment of tepsin to TGN membranes. Together, these data uncover one mechanism by which AP4 interacts with tepsin and further suggest the presence of at least one additional binding site on AP4 for tepsin in cells.

Results

β4 appendage domain binds a conserved hydrophobic motif in the tepsin C-terminus

Previous work demonstrated the β4 C-terminal appendage domain interacts directly with full-length GFP-tagged tepsin [30]. In other interactions between APs and epsins, the unstructured epsin C-terminus harbors one or more short amino acid motifs that directly bind an AP appendage domain. We created a panel of short GST-tagged fusion constructs corresponding to unstructured regions of tepsin; this included the region between the ENTH and VHS-like folded domains, as well as short regions of the entire C-terminus (Figure 1B). GST pulldown experiments using these recombinant purified GST-tepsin and β4 appendage domain constructs identified a stretch of ~50 amino acid residues in the tepsin C-terminus (residues 450–500) that binds β4 *in vitro* (Figure 1B). This interaction was visible by Coomassie staining on an SDS-PAGE gel and was further confirmed using an antibody raised specifically against β4 [21] (Figure 1B). A longer construct containing tepsin residues

450–525 also exhibited binding to β4 appendage domain but was pulled down to a lesser degree; this construct was unstable and prone to proteolysis, so we did not pursue it further, since the shorter fragment exhibited strong binding to β4. We then performed a sequence alignment of this region of tepsin across species and identified a highly conserved stretch of 8 amino acids (Figure 2A). We hypothesized this sequence, LFxG[M/L]x[L/V], might constitute a unique motif that allows tepsin to bind specifically to β4. To test this hypothesis, we used isothermal titration calorimetry (ITC) to test directly whether β4 appendage domain could bind both to a short peptide (SSRDSLFAGMELVACS) containing just the motif (Figure S1) and to a recombinant tepsin fragment containing the motif (residues 450–500). In both cases, β4 binds the tepsin sequence (Figure S1, 2B) with 1:1 stoichiometry and a low micromolar affinity (K_D= 2.9±0.8 μM, 10 independent experiments), which is typical of the strength of interactions between APs and accessory proteins [42]. This interaction is specific to β4, because neither the β1 or β2 appendage domains bind the motif *in vitro* (Figure 2B).

Using site-directed mutagenesis and ITC, we next tested whether highly conserved residues within the putative motif were key in β4 binding. All tepsin point mutants were expressed as GST-fusion proteins and purified from *E. coli*; the GST tag was removed prior to all ITC runs so that binding was conducted on untagged and unlabeled proteins. We introduced double point mutations in order to observe an effect *in vitro*; a requirement to introduce two mutations suggests a large interface and multiple side chains are involved in binding. Each of our tepsin point mutants exhibited either significantly reduced or abolished measurable binding by ITC (K_D >300 μM) (Figure 2C, 2D). The most highly conserved residues in the motif are L470, F471, G473, and M474. Simultaneous mutation of both L470 and F471 to serine residues completely abrogated binding, suggesting these residues form important hydrophobic interactions with the surface of β4. The highly conserved glycine may suggest a position in the motif at which backbone flexibility or a unique backbone conformation is required, since glycine can adopt backbone torsion angles forbidden to other amino acids. Introducing a bulkier isoleucine side chain at the glycine position, together with a polar glutamine residue in place of the conserved methionine (G473I/M474Q), also completely abrogates measurable binding. Mutating less conserved hydrophobic residues (L476S/V477S) has only a modest effect on binding: this mutant exhibits ~15-fold weaker binding. Combining the L476S mutation with a point mutant having a charged aspartate at the methionine position (M474D/L476S) substantially reduces binding, suggesting the methionine forms important contacts with β4.

The Network Protein Sequence Analysis secondary structure prediction algorithm [43] suggested the tepsin motif may form a helix, which is reminiscent of the induced helix found in a $[DE]_nX_{1–2}$FXX[FL]XXXR motif when it binds the β2 appendage domain (see below and Discussion) [41]. In the tepsin motif, the spacing of critical conserved residues identified via sequence alignment and confirmed by mutagenesis does not seem to fit the register required for a helix, so we further tested the possibility of helix induction using circular dichroism (CD) spectroscopy. Formation of the β4-tepsin complex did not exhibit any additional α-helical character (Figure S2), beyond that already present in the two isolated molecules. Combined with our mutagenesis data, this suggests the tepsin motif does not adopt a helical conformation when bound to β4 but instead may bind in an extended

conformation on the surface of β4 appendage; however, additional structural data will be required to confirm this prediction.

Chemical shift NMR data reveal the tepsin binding surface on β4 appendage domain

We next set out to identify residues on the surface of β4 appendage that bind the tepsin motif. All attempts to crystallize the β4 appendage, alone or together with a peptide corresponding to the tepsin motif, failed. Because there is an unpublished nuclear magnetic resonance (NMR) structure of β4 deposited in the PDB (2MJ7), we instead turned to NMR to identify the binding site experimentally. A NMR chemical shift perturbation (CSP) experiment was conducted monitoring changes in the ^{15}N-^{1}H heteronuclear single quantum correlation (HSQC) spectrum of ^{15}N-labeled β4 appendage domain upon titration with unlabeled tepsin (residues 450–500). The chemical shift assignments for free tepsin were obtained from the Biological Magnetic Resonance Bank (BMRB). Assignments for the complex were transferred by following the chemical shift changes over the course of the titration for signals exhibiting fast exchange on the NMR chemical shift time scale, and on the basis of the closest new signal for signals in the intermediate to slow exchange regime. Observation of signals in the intermediate and slow exchange regimes is consistent with the K_D value in the low micromolar range as measured by ITC [44]. The spectrum obtained at a 2:1 molar ratio of tepsin:4 was used to identify those peaks with substantial CSPs (Figure 3A). The analysis revealed ~20 peaks with substantial CSPs ($\delta\Delta$ (^{15}N) > 0.5 ppm, $\delta\Delta(^{1}H)$ > 0.05 ppm). To visualize the binding site on the β4 appendage, the large CSPs were mapped onto the NMR structure (Figure S3A).

We also compared the β4 structure with X-ray crystal structures of β2 appendage domain alone and in the presence of the $[DE]_nX_{1-2}FXX[FL]XXXR$ motif (PDB ID: 2G30) found in epsin1, ARH, and arrestin. β4 appendage is distinct among β appendages in having only one of the two subdomains found in other appendage domains [2–4]: β4 possesses the C-terminal platform subdomain but lacks the N-terminal sandwich subdomain. Structure conservation mapping in ConSurf (Figure S3B) highlighted specific residues in a binding patch that are highly conserved between the two domains. In addition, many of the same β4 residues found in this patch were independently identified in our NMR experiments as being critical for binding the tepsin motif. We superposed a representative conformer of the β4 NMR ensembles (PDB ID: 2MJ7) onto the β2 crystal structure (Figure S3C). The NMR structure confirms that residues 618–739 comprise the β4 appendage domain; residues prior to 618 are present in the construct but are disordered in the NMR structure. β4 superposes on the β2 platform subdomain with an RMSD of 1.9 Å in CCP4MG [45]. Furthermore, spatially equivalent residues in β2 mediate binding to the $[DE]_nX_{1-2}FXX[FL]XXXR$ motif through the F and FL pockets [41] that accommodate crucial hydrophobic residues in the motif. It thus seemed likely the tepsin motif binds β4 in an equivalent position to $[DE]_nX_{1-2}FXX[FL]XXXR$ motif binding on β2, though there are subtle structural differences between the two appendage domains (see Discussion). Based on our NMR chemical shift data and residues conserved between the β2 and β4 binding pockets, we selected several candidate β4 residues for structure-based mutagenesis: E632, W635, L636, I669, A670, and Y682 (Figure 3B, C). W635, I669, and A670 are equivalent to β2 W841, I876 and A877 in the F pocket, while Y682 is equivalent to β2 Y888 in the FL pocket. E632

and L636 are not conserved between β4 and β2 but demonstrated large chemical shift perturbations.

We then used a combination of pulldowns and ITC to test the importance of these β4 residues for binding tepsin (Figure 4). All β4 mutants used in pulldown or ITC experiments were determined to be folded using a combination of gel filtration profiles (data not shown) and CD spectroscopy (Figure S4). Our ITC and pulldown data indicate the most important residues for binding tepsin are I669, A670, and Y682. In contrast, the E632A/L636A mutant bound the tepsin motif as strongly as wild-type (data not shown). Although this suggests the glutamate and leucine residues do not interact directly with the motif but move out of the way to accommodate tepsin binding, high resolution structural data will be required to confirm this. In contrast, the I669A/A670S double mutant exhibited no measurable binding by ITC (Figure 4A). We replaced the bulky tyrosine side chain at Y682 with a smaller valine moiety; although this mutant was folded, we did not obtain enough material to undertake ITC experiments. Instead, pulldowns with the GST-tepsin fragment confirm this single point mutation is sufficient to substantially weaken binding in a pulldown assay (Figure 4B, C). Finally, we attempted to test the role of W635 because its equivalent residue in the β2 appendage is an important component of the F pocket. In β4, this residue exhibited only a small chemical shift perturbation upon the addition of tepsin. Unfortunately, our W635A mutant was completely insoluble when expressed in *E. coli*, suggesting this mutant was unfolded. In the absence of a high resolution structure, we cannot rule out the importance of this residue in binding the tepsin motif, but the small chemical shift perturbation may suggest it is not as important as other residues, in contrast to its equivalent residue in β2 appendage that plays a key role in recognizing $[DE]_nX_{1-2}FXX[FL]XXXR$ motifs.

Mutation of key residues in β4 appendage domain or the C-terminal tepsin motif disrupts the interaction between tepsin and AP4 in cultured cells

Based on our *in vitro* characterization of the tepsin binding surface on the β4 appendage domain, we sought to test the functional relevance of this interaction in cultured human cells. To provide a clean background for expression of structure-based point mutants, we used clustered, regularly interspaced, short palindromic repeat (CRISPR) technology to inactivate all alleles of *AP4B1* in HeLa M cells. Knockout of *AP4B1* was confirmed by Western blotting and sequencing (Figure 5A and S5A). Patient studies have shown that disruption of one AP4 subunit can lead to reduced expression of the others [25,27,30]. Similarly, there is a reduction in the amount of AP4 ε in the β4 knockout cell line (Figure 5A). However, as is also the case in AP4 patient cell lines, there is no change in tepsin expression level. In immunofluorescence analysis of wild-type cells, tepsin has a punctate pattern in the TGN region that co-localizes extensively with AP4 (Figure 5B; [30]). As expected, this pattern is absent in the β4 knockout cells; tepsin appears to be purely cytosolic, demonstrating that tepsin depends on AP4 for membrane recruitment (Figure 5B).

In order to test whether residues I669, A670, and Y682 in the β4 appendage domain are important for tepsin binding *in vivo*, we created stable rescue cell lines on the β4 knockout background, using either full-length wild-type β4 or one of several mutants: earless (residues 1–612); I669A/A670S; and Y682V. The earless mutant lacked the entire β4 appendage

domain and was used to determine whether the β4 appendage domain is necessary for tepsin recruitment by AP4. We immunoprecipitated AP4 from extracts of these cells with antibodies against either β4 or ε, and we determined how much tepsin co-immunoprecipitated by Western blotting (Figure 6A). Immunoprecipitates from knockout cells rescued with full-length wild-type β4 contained a similar amount of tepsin to immunoprecipitates from original wild-type parental HeLa cells. In contrast, substantially less tepsin co-immunoprecipitated with AP4 from all three mutant cell lines. The amount of tepsin in the immunoprecipitates from the I669A/A670S and Y682V cells was comparable to that from the earless cells, providing evidence that these residues are crucial for the direct interaction between tepsin and the β4 appendage domain *in vivo*. However, a small amount of tepsin still came down with AP4 in the immunoprecipitates from all three cell lines rescued with mutant β4. This is in contrast to the β4 knockout cell line where no tepsin could be detected in the AP4 immunoprecipitates, and strongly suggests the existence of at least one additional tepsin binding site elsewhere on the AP4 complex. The β4 constructs in the four rescue cell lines were expressed at similar levels (Figure S5B) and blots of the immunoprecipitates probed with antibodies against β4 and ε confirmed that immunoprecipitation of the AP4 complex was equally efficient from all four rescue cell lines (Figure 6A).

To confirm the role of the C-terminal tepsin motif (LFxG[M/L]x[L/V]) *in vivo*, we created stable HeLa cell lines expressing either wild-type tepsin C-terminally tagged with GFP (tepsin-GFP), or a tepsin-GFP construct carrying two point mutations, L470S and F471S, which had been shown to abolish binding to the β4 appendage domain *in vitro*. Immunoprecipitation of AP4 using an antibody against β4 from each cell line was performed, and co-immunoprecipitation of tepsin-GFP was assayed by probing Western blots with anti-GFP (or anti-tepsin; data not shown). These experiments demonstrated greatly reduced co-immunoprecipitation of mutant tepsin-GFP relative to wild-type tepsin-GFP (Figure 6B), supporting an important role for the C-terminal tepsin motif in binding to AP4. However, the interaction between L470S/F471S mutant tepsin-GFP and AP4 was not completely abolished, providing further evidence to support the existence of one or more additional tepsin-AP4 interaction sites.

Finally, we tested whether the interaction between β4 appendage and the C-terminal tepsin motif is necessary for the recruitment of tepsin to TGN membranes. Given that disruption of this interaction site had a severe effect on tepsin binding in the immunoprecipitation assays, we hypothesized that the residual tepsin binding observed would be insufficient to mediate recruitment of tepsin. Wild-type and mutant β4 rescue cells were fixed and double-labeled with antibodies against AP4 ε and tepsin (Figure 6C). The anti-AP4 ε labeling confirmed that all three mutant β4 proteins are able to successfully form AP4 complexes on the membrane. To our surprise, punctate co-localization of AP4 ε and tepsin could be seen in the wild-type rescue cells and the three mutant cell lines, again suggesting that other parts of the AP4 complex are involved in tepsin binding and recruitment to the membrane.

Discussion

The data presented here provide molecular insight into how the AP4 β4 appendage domain interacts specifically and directly with the major AP4 accessory protein, tepsin. The low micromolar K_D, 1:1 stoichiometry, and presence of a short motif are all reminiscent of trafficking protein interactions between AP complexes and accessory proteins found in the middle layer of AP1- or AP2-containing clathrin coated vesicles (CCVs). AP4 forms a non-clathrin coat but seems to have adopted similar strategies for interacting with accessory proteins. However, the tepsin motif binds specifically to β4 appendage and not to β appendages found in the clathrin adaptors AP1 or AP2. One notable feature of the β4 appendage domain is that it possesses only one subdomain; most other appendages, and all other β appendages, contain both an N-terminal sandwich and C-terminal platform subdomain [2–4], while β4 contains only the platform subdomain. The sandwich subdomain of AP2 β2 provides a second binding site for [FL]xxG[FL]xDF motifs found in eps15 [46]. Thus, β2 harbors 'top' and 'side' binding sites for multiple motifs in different proteins. In contrast, because β4 lacks the sandwich subdomain, it lacks an equivalent 'side' binding site for other accessory proteins. This suggests the predominant role of β4 appendage domain may be to recruit tepsin by binding the LFxG[M/L]x[L/V] motif.

The surface patch we identified on β4 is broadly conserved with the β2 patch that interacts with the $[DE]_nX_{1-2}$FXX[FL]XXXR helical motif found in epsin1, ARH, and arrestin. The two surface patches share several conserved residues, including β4 W635, I669, A670, and Y682 (equivalent to β2 residues W841, I876, A877, andY888). In 2, Y888 and W841 are located in the F and FL pockets, respectively, that accommodate critical hydrophobic residues in the $[DE]_nX_{1-2}$FXX[FL]XXXR motif. How then can we explain the specificity of the tepsin motif for β4, as observed in our ITC data? Despite very similar overall folds, the shape of the β2 and β4 surfaces differs in one important feature: β2 appendage features a deep pre-formed groove (Figure S3B) that can accommodate the helical motif. In contrast, the β4 surface is relatively flat (Figure S3C). Together with our CD data and the motif pattern, these relatively subtle differences in surface shape further support the idea that the tepsin motif likely binds β4 in an extended conformation.

Comparison of the β2 and β4 platform binding interfaces suggests that evolution modified a conserved binding patch in order to "tune" specificity for AP binding partners at different membranes. The tepsin motif is mostly hydrophobic; appears to lack key charged residues; and likely binds in an extended conformation. In contrast, the β2-binding $[DE]_nX_{1-2}$FXX[FL]XXXR motif combines an important charged moiety with key hydrophobic residues and adopts a helical conformation. Despite having similar overall three-dimensional folds and conserved residues, β2 and β4 use shape to discriminate easily between their respective epsins. This is even more important for the AP1 β1 appendage domain, since both AP1 and AP4 mediate different trafficking pathways from the TGN.

One important question is whether or not the LFxG[M/L]x[L/V] motif we have identified in tepsin is found in other proteins. To address this question, we used the Genome Net Motif [47] online search tool with the KEGG GENES database to search for other human proteins containing our motif. We obtained fifty nine hits, and we scanned the entries for motifs

located in the C-termini of these proteins. Interesting candidates included transmembrane proteins such as solute carrier family members that mediate membrane transport; subunits of the vacuolar ATPase; and a transporter implicated in Niemann-Pick disease. In the future, it will be important to test these candidate proteins to determine if they can interact with AP4.

Our data in HeLa cells suggest the LFxG[M/L]x[L/V] motif binding to β4 appendage domain is one mechanism for tepsin to bind AP4 *in vivo*. Specific disruption of this interaction, by mutation of either tepsin or β4, results in a large reduction in the amount of tepsin co-immunoprecipitated with AP4. However, it does not completely abolish the association of tepsin with AP4, suggesting the existence of at least one further interaction between AP4 and tepsin. This is also supported by immunofluorescence data from our β4 rescue cell lines: cells lacking the β4 appendage or β4 appendage mutants that cannot bind tepsin *in vitro* by ITC or IP still exhibit significant tepsin membrane recruitment. While preparing this manuscript, Mattera et al. [48] independently used yeast two-hybrid screening to identify the LFxG[M/L]x[L/V] motif in tepsin. In addition, their peptide screen identified a second tepsin binding motif, S[A/V]F[S/A]FLN, that binds the AP4 appendage domain. The presence of this second motif may explain why tepsin is still recruited to membranes in our β4 knockout and mutant rescue cell lines. However, in cells, the reported low micromolar affinity (3 μM [48]) between S[A/V]F[S/A]FLN and the ε appendage would likely be insufficient to recruit tepsin on its own. Furthermore, we note that β4 is more highly expressed in our rescue cell lines than in the parental wild-type HeLa cell line (see Figure S5B). In other experiments not discussed here, we have observed that overexpression of one AP4 subunit is sufficient to drive increased AP4 membrane recruitment and vesicle formation. This might explain how tepsin is still recruited to membranes in the mutant β4 rescue cell lines: with more AP4 present on membranes, a weaker second tepsin-AP4 interaction may be sufficient for tepsin recruitment. Alternatively, there may be additional interactions between tepsin and AP4 that have not yet been identified. For example, Mattera et al. [48] also found that deleting the tepsin ENTH and VHS-like domains together greatly reduced binding to AP4 in cell lysates, while deleting only the ENTH domain had no effect.

Our data have important implications for the role of tepsin in AP4 coat assembly and in understanding both AP4 cell biology and disease pathogenesis. AP4 is distinct among AP complexes in lacking a structural or scaffolding protein like clathrin. This raises the mechanistic question of how AP4 coats assemble, since they are unlikely to form a layered coat in the absence of clathrin. Furthermore, tepsin and AP4 are found or lost concomitantly together in eukaryotes [29], and tepsin depends upon AP4 for its membrane recruitment [30]. This suggests a strong interaction between these two proteins across evolutionary history. What then is the role of tepsin in an AP4 coat? Tepsin may be a cargo adaptor; both ENTH [36,49] and VHS [50] domains fulfill this role in other trafficking proteins, including epsins and the monomeric GGA coats. Another possibility is that tepsin may be a structural component that is required to polymerize AP4 complexes, especially in the absence of a structural or scaffolding protein. Indeed, tepsin could fulfill both of these roles simultaneously. We have accounted for only a small portion of tepsin, and much work remains to be done to understand its full role in the cell.

Materials and methods

Reagents

Unless otherwise noted, all chemicals were purchased from Sigma (St. Louis, MO, USA). The following antibodies were used in this study: rabbit anti-AP4 β, rabbit anti-AP4 ε (for western blotting and immunoprecipitation; both in-house; Hirst et al., 1999), mouse anti-AP4 ε (for immunofluorescence; 612019; BD Transduction Labs), rabbit anti-clathrin (in-house; Simpson et al., 1996), rabbit anti-GFP (gift from Matthew Seaman, Cambridge Institute for Medical Research, UK), and rabbit anti-tepsin (in-house; Borner et al., 2012). Horseradish peroxidase (HRP)–conjugated secondary antibodies were purchased from Sigma-Aldrich, and fluorescently labelled secondary antibodies were from Invitrogen. For Western blotting of immunoprecipitates where the protein band of interest was close to an IgG band, protein-A-HRP (BD Biosciences) was used in the place of HRP-conjugated secondary antibody.

Molecular biology and cloning

For structural and biochemical analyses, part of the tepsin C-terminus (residues 450–500) was subcloned into the pGEX-6P-1 backbone (GE Healthcare) using BamHI/SalI sites, to create a N-terminal GST tagged protein. β4 appendage domain (residues 612–739) was subcloned into the pGEX-4T-2 backbone (GE Healthcare) using BamHI/NotI sites, resulting in a N-terminal GST tagged protein. A two-stage quick-change mutagenesis protocol adapted from Wang and Malcolm (1999) was used to introduce mutations in the tepsin motif and the β4 appendage domain. Briefly, mutagenic primers (Sigma) were created for the desired mutations. In the first step, two PCR reactions, with either the mutagenic 5’ or 3’ primer, amplified around the plasmid. The two reactions were then combined in an additional PCR step, followed by a DpnI digest and transformation. Resultant colonies were sequenced to confirm mutagenesis.

To generate the constructs for the AP4 β rescue cell lines, full length (residues 1–739) and earless (1–612) AP4B1 were amplified by PCR from a full-length IMAGE clone of β4 (2906087). Cloning sites were added (5’ SalI and 3’ NotI), and the PCR products were cloned into a modified version of the retroviral expression vector pLXIN (gift from Andrew Peden, University of Sheffield, UK). Full length pLXIN_AP4B1 was modified by site-directed mutagenesis to give pLXIN_AP4B1[Y682V] and pLXIN_AP4B1[I669A/A670S], as described above. For the tepsin-GFP mutant, the L470S and F471S point mutations were introduced into a tepsin-GFP plasmid reported previously [30] by site-directed mutagenesis. Wild-type and mutant tepsin-GFP were subsequently amplified by PCR from the wild-type and mutant tepsin-GFP plasmids, respectively, and were inserted into the HpaI site of the modified pLXIN vector using Gibson Assembly Master Mix (New England Biolabs)-directed cloning. The sequences of all constructs described here were verified by Sanger DNA sequencing.

GST pulldown assays

GST or GST-tepsin proteins (50 μg) were immobilized on glutathione sepharose resin for 1 hour on ice. The resin was incubated for 2 hours on ice with wild-type or Y682V β4 (75 μg)

in 20 mM HEPES (pH 7.5), 200 mM NaCl, and 2 mM DTT, with additional buffer added at 1 hour. Samples were washed three times with the same buffer plus 1 mM EDTA and 0.1% v/v Triton X-100. Proteins were eluted from the resin using the wash buffer plus 30 mM reduced glutathione following a 30 minute incubation on ice. Gel samples were prepared from the supernatant following elution, and the assay was analyzed by Coomassie staining of SDS-PAGE gels. When gels were further analyzed by Western blotting, rabbit anti-AP4 β antibody [21] was used.

Protein expression and purification

Constructs were expressed in BL21(DE3)pLysS cells (Invitrogen) for 16–20 hr at 22°C after induction with 0.4 mM IPTG. Wild-type β4 appendage domain and all tepsin constructs were purified in 20 mM HEPES (pH 7.5), 200 mM NaCl, and 2 mM βME. Mutant β4 appendage domain constructs were purified in 20 mM HEPES (pH 7.5), 500 mM NaCl, and 2 mM βME. Cells were lysed by a disruptor (Constant Systems Limited, Daventry, UK), and proteins were affinity purified using glutathione sepharose (GE Healthcare) in the purification buffer. GST-tagged β4 appendage domains were cleaved overnight with thrombin (Recothrom, The Medicines Company, Parsippany, NJ) at room temperature and eluted in batch. GST-tagged tepsin was cleaved overnight with recombinant 3C protease at 4°C and eluted in batch. All proteins were further purified by gel filtration on a Superdex S200 preparative or analytical column (GE Healthcare).

NMR titration experiments

Uniformly enriched ^{15}N-labelled β4 appendage domain was produced in minimal media (M9) with 0.5g/L $^{15}NH_4Cl$ (Cambridge Isotope Laboratory) as the sole nitrogen source. Otherwise, expression and purification proceeded as described above. Samples were prepared in gel filtration buffer with 10% v/v D_2O at a concentration of 300 μM. Unlabeled tepsin was added in 0.1 or 0.3 mol equivalents until a 2:1 tepsin:β4 ratio was reached. Standard 2D ^{15}N-^{1}H HSQC NMR spectra were collected at 25°C on a 600 MHz Bruker Avance III spectrometer with a TCI triple resonance cryoprobe (Bruker BioSpin). Data were processed initially using TopSpin 3.2 (Bruker BioSpin), with linear prediction in the indirect dimension plus one-fold zero filling, and squared sine bell apodization in both dimensions. The full titration was further analyzed using NMRViewJ (Version 8.0.3, One Moon Scientific). Resonance assignments for β4 were obtained from the BMRB database (19709) and were transposed to our HSQC spectra manually. To analyze the titration data, peaks were classified as did not move, moved slightly (detectable but ≤ 0.5 ppm in ^{15}N or ≤ 0.05 ppm in ^{1}H), or moved greatly (> 0.5 ppm in ^{15}N or ≤ 0.05 ppm in ^{1}H).

Isothermal titration calorimetry

ITC experiments were conducted on a NanoITC instrument (TA Instruments) at 20°C. Molar peptide concentration in the syringe was at least 6.25 times that of protein in the cell. In experiments using the synthetic tepsin peptide, β4 appendage domain constructs were gel filtered into 50 mM HEPES (pH 7.5), 100 mM NaCl, and 0.5 mM TCEP. In experiments using recombinant tepsin, β4 appendage and tepsin constructs were gel filtered into 20 mM HEPES (pH7.5), 100 mM NaCl, and 0.5 mM TCEP. Incremental titrations were performed with either initial baseline of 180s and injection intervals of 180s, or initial baseline of 120s

and injection intervals of 250s. Titration data were analyzed in NanoAnalyze (TA Instruments) to obtain a fit and values for stoichiometry (n) and equilibrium association constant (K_a).

Circular dichroism

Spectra were collected on a Jasco J-810 CD spectropolarimeter, using a cell with 1 mm pathlength. Protein samples were diluted to 0.1 mg/ml in MilliQ water. Data was collected with standard sensitivity, scanning from wavelengths of 260 to 190 nm with a data pitch of 1 nm or 0.5 nm. Under continuous scanning mode the scan speed was 100 nm/min with a response time of 2s, and 5 accumulations were collected.

CRISPR knockout of AP-4 β subunit

We inactivated all copies of the *AP4B1* gene in HeLa M cells using the 'double nickase' CRISPR/Cas9 system [51,52]. This system minimises the off-target effects associated with the use of wild-type Cas9 by using a mutant Cas9 enzyme (D10A) which can only make single-strand breaks. In combination with paired guide RNAs (gRNAs), this allows the specific introduction of a compound double-strand break at a site of interest. The Zhang online CRISPR design tool (http://crispr.mit.edu/, [53]) was used to identify suitable paired gRNA targets in *AP4B1*: GACCCCAATCCAATGGTGCG and TGCACAGCGTATTGATGGCC (both in exon 2 of transcript ENST00000369569). Each gRNA was ordered as a pair of complementary oligos with the sequences 5'CACCG$N_{19/20}$-3' and 5'AAAC$N_{19/20}$C-3'. Due to the requirement of the human U6 promoter for a G at the transcriptional start site, an extra G was added in front of the second gRNA target sequence. Oligo pairs were annealed and cloned into the BbsI site of pX335 (Addgene). HeLa M cells were transfected with both pX335 plasmids and pIRESpuro (Clontech) in a ratio of 2:2:1 using a TransIT-HeLaMONSTER transfection kit (Mirus Bio LLC). Forty-eight hours later, untransfected cells were killed off by a 4 day selection in 1 μg/ml puromycin. Single cell clones were isolated by serial dilution of the cells and tested for knockout of AP4 β by Western blotting and immunofluorescence. Clone x2A3 was negative for AP4 β expression in both assays and was further validated by sequencing. Genomic DNA was harvested using a High Pure PCR Template Purification Kit (Roche) and PCR was used to amplify a 633 base pair region around the target sites. The PCR products were then blunt-end cloned (Zero Blunt PCR Cloning Kit; Invitrogen) and 24 clones were sent for Sanger sequencing with the M13_F primer (Beckman Coulter Genomics).

Cell lines and tissue culture

HeLa M [54] cells were maintained in RPMI 1640, supplemented with 10% v/v foetal calf serum (FCS), 100 units/ml penicillin, and 100 μg/ml streptomycin. Stable cell lines were additionally maintained with 500 μg/ml G418 (PAA). Stable cell lines were created using retrovirus made in HEK 293ET cells transfected using TransIT-293 Transfection Reagent (Mirus Bio LLC). pLXIN plasmids were mixed with the packaging plasmids pMD.GagPol and pMD.VSVG in a ratio of 10:7:3. Viral supernatants were harvested after 48 hours and used to transduce HeLa M (for the tepsin-GFP cell lines) or HeLa AP4 β knockout clone

x2A3 (for the AP4 β rescue cell lines) cells. Transduced cells were selected in 500 μg/ml G418 48 hours post-transduction.

Fluorescence microscopy

Cells were grown onto 13 mm glass coverslips and fixed in ice-cold methanol. Fixed cells were blocked in 0.5 % bovine serum albumin (BSA; in PBS [137 mM NaCl, 2.7 mM KCl, 10 mM Na2HPO4, and 1.76 mM KH2PO4, pH 7.4]). Primary antibody (diluted in BSA block) was added for 45 minutes at room temperature. Coverslips were washed three times in BSA block and then fluorochrome-conjugated secondary antibody was added in block for 30 minutes at room temperature. Coverslips were then washed three times in PBS, followed by a final wash in dH_2O, before being mounted in ProLong Gold Antifade Reagent (Life Technologies). Antibody fluorescence was visualised with an Axio Imager II microscope (Carl Zeiss), controlled by AxioVision software (Carl Zeiss).

Immunoprecipitations and Western blotting

Estimations of protein concentrations were made using a Pierce BCA Protein Assay Kit (Thermo Fisher Scientific). For immunoprecipitations of AP4 β and AP4 ε, cells in 100 mm plates were lysed in 1 ml 1% Triton TX-100 (in PBS), supplemented with 200 μM AEBSF protease inhibitor. Lysates were cleared by centrifugation and, if required, lysates were adjusted to the same concentration with 1% Triton TX-100. A portion of each lysate was retained as input and the remainder pre-cleared by incubation with 30 μl packed protein-A-sepharose (GE Healthcare) for 1 hour. To each pre-cleared lysate, 5 μl antibody were added for 3 hours incubation and then 30 μl packed protein-A-sepharose were added to recover immunoprecipitated complexes. The sepharose was then washed three times with 1% Triton TX-100, two times with PBS, and boiled in NuPAGE LDS Sample Buffer (Life Technologies) to prepare for Western blot analysis.

Unless prepared for immunoprecipitation, cells were lysed for Western blot analysis in 2.5% (wt/vol) SDS/50 mM Tris, pH 8.0. Lysates were passed through a QIAshredder column (Qiagen) to shred DNA, incubated at 65 °C for 3 minutes, and then boiled in NuPAGE LDS Sample Buffer. Samples were loaded at equal protein amounts for SDS-PAGE, performed on NuPAGE 4–12% Bis-Tris gels in NuPAGE MOPS SDS Running Buffer (Life Technologies). PageRuler Plus Prestained Protein Ladder (Thermo Scientific) was used to estimate the molecular size of bands. Proteins were transferred to nitrocellulose membrane by wet transfer and membranes were blocked in 5% w/v milk in PBS with 0.1% v/v Tween-20 (PBS-T). Primary antibodies (diluted in 5% milk) were added for at least 1 hour at room temperature, followed by washing in PBS-T, incubation in secondary antibody (also in 5% milk) for 30 minutes at room temperature, washing in PBS-T, and finally PBS. Chemiluminescence detection of HRP-conjugated secondary antibody/protein-A was carried out using Amersham ECL Prime Western Blotting Detection Reagent (GE Healthcare) and X-ray film.

Supplementary Material

Refer to Web version on PubMed Central for supplementary material.

Acknowledgments

The authors thank Linton Traub for the β1 construct; Kate Mittendorf for helpful NMR discussions; and David Owen for the β2 construct, helpful discussion, and critical reading of the manuscript. LPJ and MNF are supported by funds from Vanderbilt University College of Arts and Science to LPJ. MNF is supported on a Molecular Biophysics Training Grant (NIH 5T32GM008320). AKD and MSR are supported by a Wellcome Trust Principal Research Fellowship to MSR. AKD is supported by a National Institute for Health Research Cambridge Biomedical Research Centre PhD Fellowship. GHHB is supported by the Max Planck Society for the Advancement of Science. NMR instrumentation is supported in part by grants from the NSF (0922862), NIH (S10 RR025677), and Vanderbilt University matching funds.

References

1. Owen DJ, Evans PR. A structural explanation for the recognition of tyrosine-based endocytotic signals. Science (80-) [Internet]. 1998; 282:1327–1332. Available from: http://www.ncbi.nlm.nih.gov/pubmed/9812899.
2. Owen DJ, Vallis Y, Noble MEM, Hunter JB, Dafforn TR, Evans PR, McMahon HT. A Structural Explanation for the Binding of Multiple Ligands by the α-adaptin Appendage Domain. Cell. 1999; 97:805–815. [PubMed: 10380931]
3. Traub LM, Downs MA, Westrich JL, Fremont DH. Crystal structure of the alpha appendage of AP-2 reveals a recruitment platform for clathrin-coat assembly. Proc Natl Acad Sci U S A [Internet]. 1999; 96:8907–8912. Available from: http://www.pubmedcentral.nih.gov/articlerender.fcgi?artid=17706&tool=pmcentrez&rendertype=abstract.
4. Owen DJ, Vallis Y, Pearse BM, McMahon HT, Evans PR. The structure and function of the β2-adaptin appendage domain. EMBO J [Internet]. 2000; 19:4216–4227. Available from: http://www.pubmedcentral.nih.gov/articlerender.fcgi?artid=302036&tool=pmcentrez&rendertype=abstract.
5. Collins BM, McCoy AJ, Kent HM, Evans PR, Owen DJ. Molecular architecture and functional model of the endocytic AP2 complex. Cell [Internet]. 2002; 109:523–535. Available from: http://www.ncbi.nlm.nih.gov/pubmed/12086608.
6. Heldwein EE, Macia E, Wang J, Yin HL, Kirchhausen T, Harrison SC. Crystal structure of the clathrin adaptor protein 1 core. Proc Natl Acad Sci U S A [Internet]. 2004; 101:14108–14113. Available from: http://www.pubmedcentral.nih.gov/articlerender.fcgi?artid=521094&tool=pmcentrez&rendertype=abstract.
7. Kelly BT, McCoy AJ, Späte K, Miller SE, Evans PR, Höning S, Owen DJ. A structural explanation for the binding of endocytic dileucine motifs by the AP2 complex. Nature [Internet]. 2008; 456:976–979. Available from: http://www.ncbi.nlm.nih.gov/pubmed/19140243.
8. Jackson LP, Kelly BT, McCoy AJ, Gaffry T, James LC, Collins BM, Höning S, Evans PR, Owen DJ. A large-scale conformational change couples membrane recruitment to cargo binding in the AP2 clathrin adaptor complex. Cell [Internet]. 2010; 141:1220–1229. Available from: http://www.ncbi.nlm.nih.gov/pubmed/20603002.
9. Kelly BT, Graham SC, Liska N, Dannhauser PN, Honing S, Ungewickell EJ, Owen DJ. AP2 controls clathrin polymerization with a membrane-activated switch. Science (80-) [Internet]. 2014; 345:459–463. Available from: http://www.sciencemag.org/cgi/doi/10.1126/science.1254836.
10. Boucrot E, Saffarian S, Zhang R, Kirchhausen T. Roles of AP-2 in clathrin-mediated endocytosis. PLoS One [Internet]. 2010; 5:e10597. Available from: http://www.pubmedcentral.nih.gov/articlerender.fcgi?artid=2868873&tool=pmcentrez&rendertype=abstract.
11. Kirchhausen T, Owen D, Harrison SC. Molecular structure, function, and dynamics of clathrin-mediated membrane traffic. Cold Spring Harb Perspect Biol [Internet]. 2014; 6 Available from: http://www.ncbi.nlm.nih.gov/pubmed/24789820.
12. Antonescu C, Aguet F, Danuser G, Schmid SL. Phosphatidylinositol-(4, 5)-bisphosphate regulates clathrin-coated pit initiation, stabilization, and size. Mol Biol Cell [Internet]. 2011; 22:2588–2600. Available from: http://www.molbiolcell.org/content/22/14/2588.short.
13. Hirst J, Borner GHH, Antrobus R, Peden Aa, Hodson Na, Sahlender Da, Robinson MS. Distinct and overlapping roles for AP-1 and GGAs revealed by the “knocksideways” system. Curr Biol [Internet]. 2012; 22:1711–1716. Available from: http://dx.doi.org/10.1016/j.cub.2012.07.012.

14. Ren X, Farías GG, Canagarajah BJ, Bonifacino JS, Hurley JH. Structural basis for recruitment and activation of the AP-1 clathrin adaptor complex by Arf1. Cell [Internet]. 2013; 152:755–767. Available from: http://www.ncbi.nlm.nih.gov/pubmed/23415225.
15. Shen Q-T, Ren X, Zhang R, Lee I-H, Hurley JH. HIV-1 Nef hijacks clathrin coats by stabilizing AP-1:Arf1 polygons. Science (80-) [Internet]. 2015; 350:aac5137. Available from: http://www.ncbi.nlm.nih.gov/pubmed/26494761.
16. Boehm M, Aguilar RC, Bonifacino JS. Functional and physical interactions of the adaptor protein complex AP-4 with ADP-ribosylation factors (ARFs). EMBO J [Internet]. 2001; 20:6265–6276. Available from: http://www.pubmedcentral.nih.gov/articlerender.fcgi?artid=125733&tool=pmcentrez&rendertype=abstract.
17. Simmen T, Höning S, Icking A, Tikkanen R, Hunziker W. AP-4 binds basolateral signals and participates in basolateral sorting in epithelial MDCK cells. Nat Cell Biol [Internet]. 2002; 4:154–159. Available from: http://www.ncbi.nlm.nih.gov/pubmed/11802162.
18. Yap CC, Murate M, Kishigami S, Muto Y, Kishida H, Hashikawa T, Yano R. Adaptor protein complex-4 (AP-4) is expressed in the central nervous system neurons and interacts with glutamate receptor delta2. Mol Cell Neurosci [Internet]. 2003; 24:283–295. Available from: http://linkinghub.elsevier.com/retrieve/pii/S1044743103001647.
19. Matsuda S, Miura E, Matsuda K, Kakegawa W, Kohda K, Watanabe M, Yuzaki M. Accumulation of AMPA receptors in autophagosomes in neuronal axons lacking adaptor protein AP-4. Neuron [Internet]. 2008; 57:730–745. Available from: http://www.ncbi.nlm.nih.gov/pubmed/18341993.
20. Burgos PV, Mardones GA, Rojas AL, DaSilva LLP, Prabhu Y, Hurley JH, Bonifacino JS. Sorting of the Alzheimer's disease amyloid precursor protein mediated by the AP-4 complex. Dev Cell [Internet]. 2010; 18:425–436. Available from: http://www.pubmedcentral.nih.gov/articlerender.fcgi?artid=2841041&tool=pmcentrez&rendertype=abstract.
21. Hirst J, Bright NA, Rous B, Robinson MS. Characterization of a fourth adaptor-related protein complex. Mol Biol Cell [Internet]. 1999; 10:2787–2802. Available from: http://www.pubmedcentral.nih.gov/articlerender.fcgi?artid=25515&tool=pmcentrez&rendertype=abstract.
22. Hirst J, Irving C, Borner GHH. Adaptor protein complexes AP-4 and AP-5: new players in endosomal trafficking and progressive spastic paraplegia. Traffic [Internet]. 2013; 14:153–164. Available from: http://www.ncbi.nlm.nih.gov/pubmed/23167973.
23. Abou Jamra R, Philippe O, Raas-Rothschild A, Eck SH, Graf E, Buchert R, Borck G, Ekici A, Brockschmidt FF, Nöthen MM, Munnich A, Strom TM, Reis A, Colleaux L. Adaptor protein complex 4 deficiency causes severe autosomal-recessive intellectual disability, progressive spastic paraplegia, shy character, and short stature. Am J Hum Genet [Internet]. 2011; 88:788–795. Available from: http://www.pubmedcentral.nih.gov/articlerender.fcgi?artid=3113253&tool=pmcentrez&rendertype=abstract.
24. Abdollahpour H, Alawi M, Kortüm F, Beckstette M, Seemanova E, Komárek V, Rosenberger G, Kutsche K. An AP4B1 frameshift mutation in siblings with intellectual disability and spastic tetraplegia further delineates the AP-4 deficiency syndrome. Eur J Hum Genet [Internet]. 2015; 23:256–259. Available from: http://www.ncbi.nlm.nih.gov/pubmed/24781758.
25. Hardies K, May P, Djemie T, Tarta-Arsene O, Deconinck T, Craiu D, Helbig I, Suls A, Balling R, Weckhuysen S, De Jonghe P, Hirst J, Afawi Z, Barisic N, Baulac S, Caglayan H, Depienne C, De Kovel CGF, Dimova P, Guerrero-Lopez R, Guerrini R, Hjalgrim H, Hoffman-Zacharska D, Jahn J, Klein KM, Koeleman BPC, Leguern E, Lehesjoki A-E, Lemke J, Lerche H, Marini C, Muhle H, Rosenow F, Serratosa JM, Moller RS, Stephani U, Striano P, Talvik T, Von Spiczak S, Weber Y, Zara F. Recessive loss-of-function mutations in AP4S1 cause mild fever-sensitive seizures, developmental delay and spastic paraplegia through loss of AP-4 complex assembly. Hum Mol Genet [Internet]. 2015:1–10. Available from: http://www.hmg.oxfordjournals.org/cgi/doi/10.1093/hmg/ddu740.
26. Tüysüz B, Bilguvar K, Koçer N, Yalçınkaya C, Çağlayan O, Gül E, Sahin S, Çomu S, Günel M. Autosomal recessive spastic tetraplegia caused by AP4M1 and AP4B1 gene mutation: expansion of the facial and neuroimaging features. Am J Med Genet A [Internet]. 2014; 164A:1677–85. Available from: http://www.ncbi.nlm.nih.gov/pubmed/24700674.

27. Hirst J, Irving C, Borner GHH. Adaptor protein complexes AP-4 and AP-5: new players in endosomal trafficking and progressive spastic paraplegia. Traffic [Internet]. 2013; 14:153–164. Available from: http://www.ncbi.nlm.nih.gov/pubmed/23167973.
28. Field MC, Gabernet-Castello C, Dacks JB. Reconstructing the evolution of the endocytic system: insights from genomics and molecular cell biology. Adv Exp Med Biol [Internet]. 2007; 607:84–96. Available from: http://www.ncbi.nlm.nih.gov/pubmed/17977461.
29. Hirst J, Schlacht A, Norcott JP, Traynor D, Bloomfield G, Antrobus R, Kay RR, Dacks JB, Robinson MS. Characterization of TSET, an ancient and widespread membrane trafficking complex. Elife [Internet]. 2014; 3:e02866. Available from: http://www.pubmedcentral.nih.gov/articlerender.fcgi?artid=4031984&tool=pmcentrez&rendertype=abstract.
30. Borner GHH, Antrobus R, Hirst J, Bhumbra GS, Kozik P, Jackson LP, Sahlender DA, Robinson MS. Multivariate proteomic profiling identifies novel accessory proteins of coated vesicles. J Cell Biol [Internet]. 2012; 197:141–160. Available from: http://www.jcb.org/cgi/doi/10.1083/jcb.201111049.
31. Ford MGJ, Mills IG, Peter BJ, Vallis Y, Praefcke GJK, Evans PR, McMahon HT. Curvature of clathrin-coated pits driven by epsin. Nature [Internet]. 2002; 419:361–366. Available from: http://www.ncbi.nlm.nih.gov/pubmed/12353027.
32. Hirst J, Motley A, Harasaki K, Peak Chew SY, Robinson MS. EpsinR: an ENTH domain-containing protein that interacts with AP-1. Mol Biol Cell [Internet]. 2003; 14:625–641. Available from: http://www.pubmedcentral.nih.gov/articlerender.fcgi?artid=149997&tool=pmcentrez&rendertype=abstract.
33. Mills IG, Praefcke GJK, Vallis Y, Peter BJ, Olesen LE, Gallop JL, Butler PJG, Evans PR, McMahon HT. EpsinR: an AP1/clathrin interacting protein involved in vesicle trafficking. J Cell Biol [Internet]. 2003; 160:213–222. Available from: http://www.pubmedcentral.nih.gov/articlerender.fcgi?artid=2172650&tool=pmcentrez&rendertype=abstract.
34. Oldham CE, Mohney RP, Miller SLH, Hanes RN, O'Bryan JP. The ubiquitin-interacting motifs target the endocytic adaptor protein epsin for ubiquitination. Curr Biol [Internet]. 2002; 12:1112–1116. Available from: http://www.ncbi.nlm.nih.gov/pubmed/12121618.
35. Hawryluk MJ, Keyel PA, Mishra SK, Watkins SC, Heuser JE, Traub LM. Epsin 1 is a polyubiquitin-selective clathrin-associated sorting protein. Traffic [Internet]. 2006; 7:262–281. Available from: http://www.ncbi.nlm.nih.gov/pubmed/16497222.
36. Miller SE, Collins BM, McCoy AJ, Robinson MS, Owen DJ. A SNARE-adaptor interaction is a new mode of cargo recognition in clathrin-coated vesicles. Nature [Internet]. 2007; 450:570–574. Available from: http://www.ncbi.nlm.nih.gov/pubmed/18033301.
37. Messa M, Fernández-Busnadiego R, Sun EW, Chen H, Czapla H, Wrasman K, Wu Y, Ko G, Ross T, Wendland B, De Camilli P. Epsin deficiency impairs endocytosis by stalling the actin-dependent invagination of endocytic clathrin-coated pits. Elife [Internet]. 2014; 3:e03311. Available from: http://www.ncbi.nlm.nih.gov/pubmed/25122462.
38. Rosenthal JA, Chen H, Slepnev VI, Pellegrini L, Salcini AE, Di Fiore PP, De Camilli P. The epsins define a family of proteins that interact with components of the clathrin coat and contain a new protein module. J Biol Chem [Internet]. 1999; 274:33959–33965. Available from: http://www.ncbi.nlm.nih.gov/pubmed/10567358.
39. Drake MT, Downs MA, Traub LM. Epsin binds to clathrin by associating directly with the clathrin-terminal domain. Evidence for cooperative binding through two discrete sites. J Biol Chem [Internet]. 2000; 275:6479–6489. Available from: http://www.ncbi.nlm.nih.gov/pubmed/10692452.
40. Praefcke GJK, Ford MGJ, Schmid EM, Olesen LE, Gallop JL, Peak-Chew S-Y, Vallis Y, Babu MM, Mills IG, McMahon HT. Evolving nature of the AP2 alpha-appendage hub during clathrin-coated vesicle endocytosis. EMBO J [Internet]. 2004; 23:4371–4383. Available from: http://www.ncbi.nlm.nih.gov/pubmed/15496985.
41. Edeling MA, Mishra SK, Keyel PA, Steinhauser AL, Collins BM, Roth R, Heuser JE, Owen DJ, Traub LM. Molecular switches involving the AP-2 beta2 appendage regulate endocytic cargo selection and clathrin coat assembly. Dev Cell [Internet]. 2006; 10:329–342. Available from: http://www.ncbi.nlm.nih.gov/pubmed/16516836.

42. Edeling MA, Smith C, Owen D. Life of a clathrin coat: insights from clathrin and AP structures. Nat Rev Mol Cell Biol [Internet]. 2006; 7:32–44. Available from: http://www.ncbi.nlm.nih.gov/pubmed/16493411.
43. Combet C, Blanchet C, Geourjon C, Deléage G. NPS@: Network Protein Sequence Analysis. TIBS. 2000; 25:147–150. [PubMed: 10694887]
44. Ziarek JJ, Peterson FC, Lytle BL, Volkman BF. Binding site identification and structure determination of protein-ligand complexes by NMR a semiautomated approach. Methods Enzym [Internet]. 2011; 493:241–275. Available from: http://www.ncbi.nlm.nih.gov/pubmed/21371594.
45. McNicholas S, Potterton E, Wilson KS. Noble MEM. Presenting your structures: the CCP4mg molecular-graphics software. Acta Cryst D [Internet]. 2011; 67:386–394. Available from: http://www.ncbi.nlm.nih.gov/pubmed/21460457.
46. Schmid EM, Ford MGJ, Burtey A, Praefcke GJK, Peak-Chew S-Y, Mills IG, Benmerah A, McMahon HT. Role of the AP2 beta-appendage hub in recruiting partners for clathrin-coated vesicle assembly. PLoS Biol [Internet]. 2006; 4:e262. Available from: http://www.ncbi.nlm.nih.gov/pubmed/16903783.
47. Kanehisa M, Goto S, Kawashima S, Nakaya A. The KEGG databases at GenomeNet. Nucleic Acids Res [Internet]. 2002; 30:42–46. Available from: http://www.ncbi.nlm.nih.gov/pubmed/11752249.
48. Mattera R, Guardia CM, Sidhu S, Bonifacino JS. Bivalent Motif-Ear Interactions Mediate the Association of the Accessory Protein Tepsin with the AP-4 Adaptor Complex. J Biol Chem [Internet]. 2015 jbc.M115.683409. Available from: http://www.jbc.org/lookup/doi/10.1074/jbc.M115.683409.
49. Hirst J, Miller SE, Taylor MJ, von Mollard GF, Robinson MS. EpsinR is an adaptor for the SNARE protein Vti1b. Mol Biol Cell [Internet]. 2004; 15:5593–5602. Available from: http://www.pubmedcentral.nih.gov/articlerender.fcgi?artid=532037&tool=pmcentrez&rendertype=abstract.
50. Misra S, Puertollano R, Kato Y, Bonifacino JS, Hurley JH. Structural basis for acidic-cluster-dileucine sorting-signal recognition by VHS domains. Nature [Internet]. 2002; 415:933–937. Available from: http://www.ncbi.nlm.nih.gov/pubmed/11859375.
51. Cong L, Ran FA, Cox D, Lin S, Barretto R, Habib N, Hsu PD, Wu X, Jiang W, Marraffini LA, Zhang F. Multiplex genome engineering using CRISPR/Cas systems. Science (80-) [Internet]. 2013; 339:819–823. Available from: http://www.ncbi.nlm.nih.gov/pubmed/23287718.
52. Ran FA, Hsu PD, Lin C-Y, Gootenberg JS, Konermann S, Trevino AE, Scott DA, Inoue A, Matoba S, Zhang Y, Zhang F. Double nicking by RNA-guided CRISPR Cas9 for enhanced genome editing specificity. Cell [Internet]. 2013; 154:1380–1389. Available from: http://www.ncbi.nlm.nih.gov/pubmed/23992846.
53. Hsu PD, Scott DA, Weinstein JA, Ran FA, Konermann S, Agarwala V, Li Y, Fine EJ, Wu X, Shalem O, Cradick TJ, Marraffini LA, Bao G, Zhang F. DNA targeting specificity of RNA-guided Cas9 nucleases. Nat Biotech [Internet]. 2013; 31:827–832. Available from: http://www.ncbi.nlm.nih.gov/pubmed/23873081.
54. Tiwari RK, Kusari J, Sen GC. Functional equivalents of interferon-mediated signals needed for induction of an mRNA can be generated by double-stranded RNA and growth factors. EMBO J [Internet]. 1987; 6:3373–3378. Available from: http://www.ncbi.nlm.nih.gov/pubmed/2828026.

Synopsis

The adaptor protein (AP) complex family mediates membrane trafficking events, but the molecular mechanisms of the non-clathrin AP4 coat remain poorly understood. We identify a conserved sequence in the AP4 accessory protein, tepsin, that directly interacts with the β4 appendage domain, and we map the tepsin binding site on the β4 surface. Mutations of key residues in the tepsin sequence or on β4 demonstrate their importance for binding both *in vitro* and in cultured cells. These data provide the first detailed molecular glimpse of how AP4 interacts with an accessory protein.

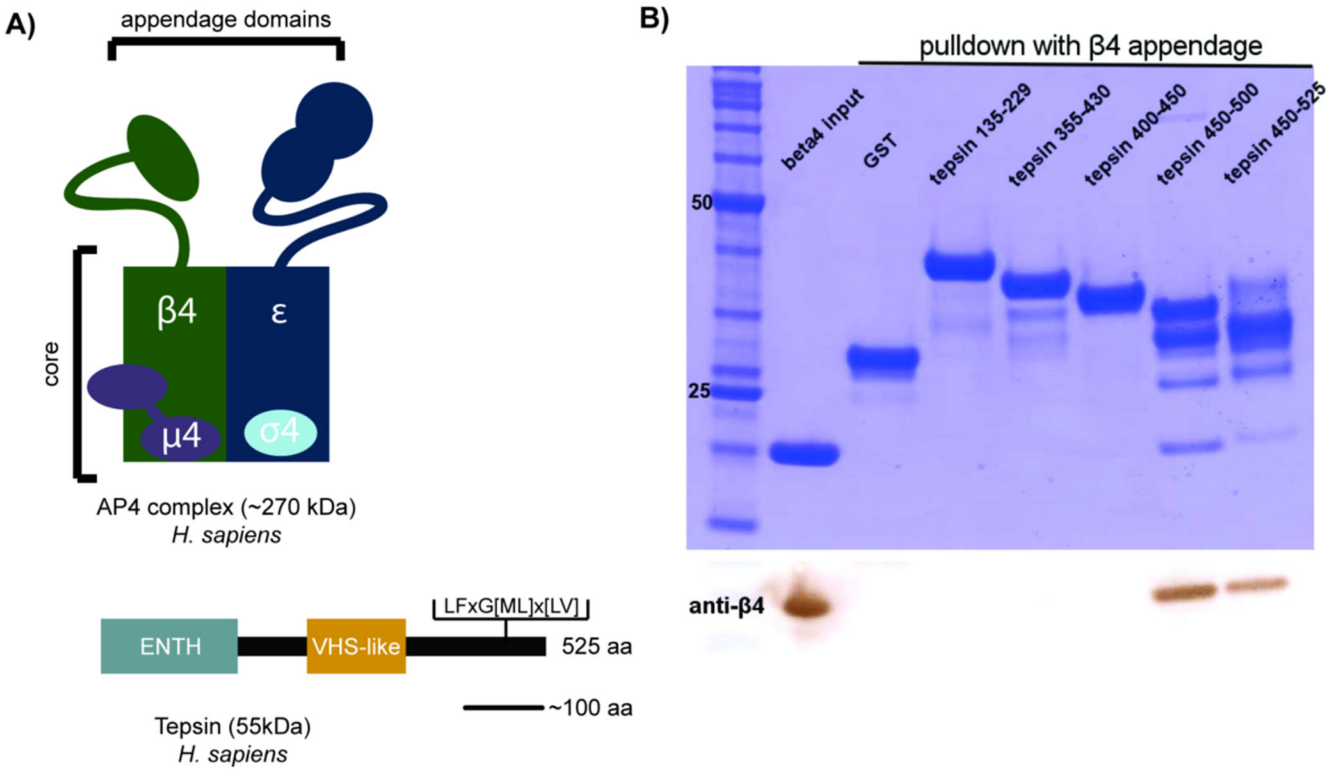

Figure 1. The AP4 β4 appendage domain interacts directly with the tepsin C-terminus

A) Schematics of AP4 coat protein complex (top, ε/β4/μ4/σ4 subunits) and tepsin (bottom). Tepsin contains structured ENTH and VHS-like domains at its N-terminus, together with a mostly unstructured C-terminus. The conserved hydrophobic sequence for binding to β4 identified in this work (LFxG[M/L]x[L/V]) is highlighted. B) Pulldown experiments using recombinant purified proteins identified a region in the tepsin C-terminus that binds β4; a panel of GST-tepsin constructs was used as bait and β4 appendage domain as prey. (Top: Coomassie-stained SDS- PAGE gel with tepsin construct amino acid residue ranges marked; bottom: Western blot using anti-β4 antibody).

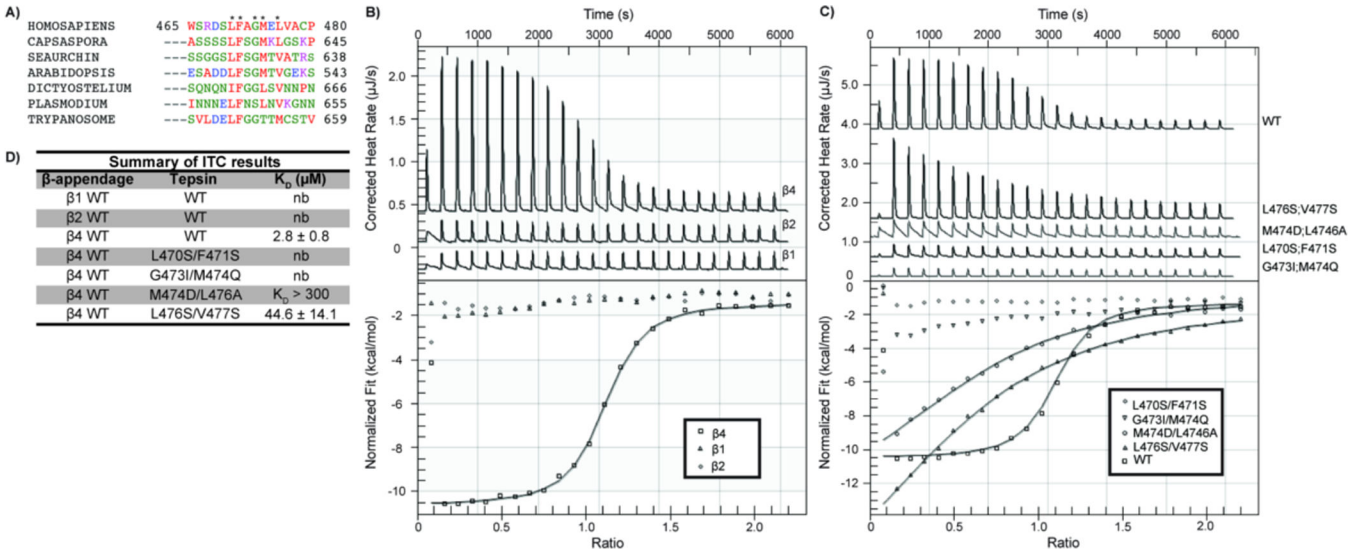

D)

Summary of ITC results		
β-appendage	Tepsin	K_D (μM)
β1 WT	WT	nb
β2 WT	WT	nb
β4 WT	WT	2.8 ± 0.8
β4 WT	L470S/F471S	nb
β4 WT	G473I/M474Q	nb
β4 WT	M474D/L476A	K_D > 300
β4 WT	L476S/V477S	44.6 ± 14.1

Figure 2. Mutagenesis of a conserved hydrophobic sequence in tepsin reduces or abolishes binding to β4

A) Sequence alignment of tepsin from major eukaryotic super groups reveals a conserved stretch of 8 residues in the unstructured C-terminus. Asterisks mark highly conserved amino acids. B) Wild-type β4 binds a recombinant tepsin fragment (residues 450–500) containing the conserved sequence with a K_D of 2.9±0.8 μM by isothermal titration calorimetry (ITC, 10 independent experiments). In contrast, the tepsin fragment cannot bind purified β1 or β2 appendages found in the clathrin adaptors AP1 or AP2, respectively. C) Representative ITC traces of tepsin mutants with WT β4. Tepsin residues marked by asterisks in A) were mutated to test their importance for binding. All mutants either reduced or abrogated measurable binding to β4 *in vitro*. D) ITC summary results table. All K_D values are represented as averages ± standard deviation; nb= no measurable binding.

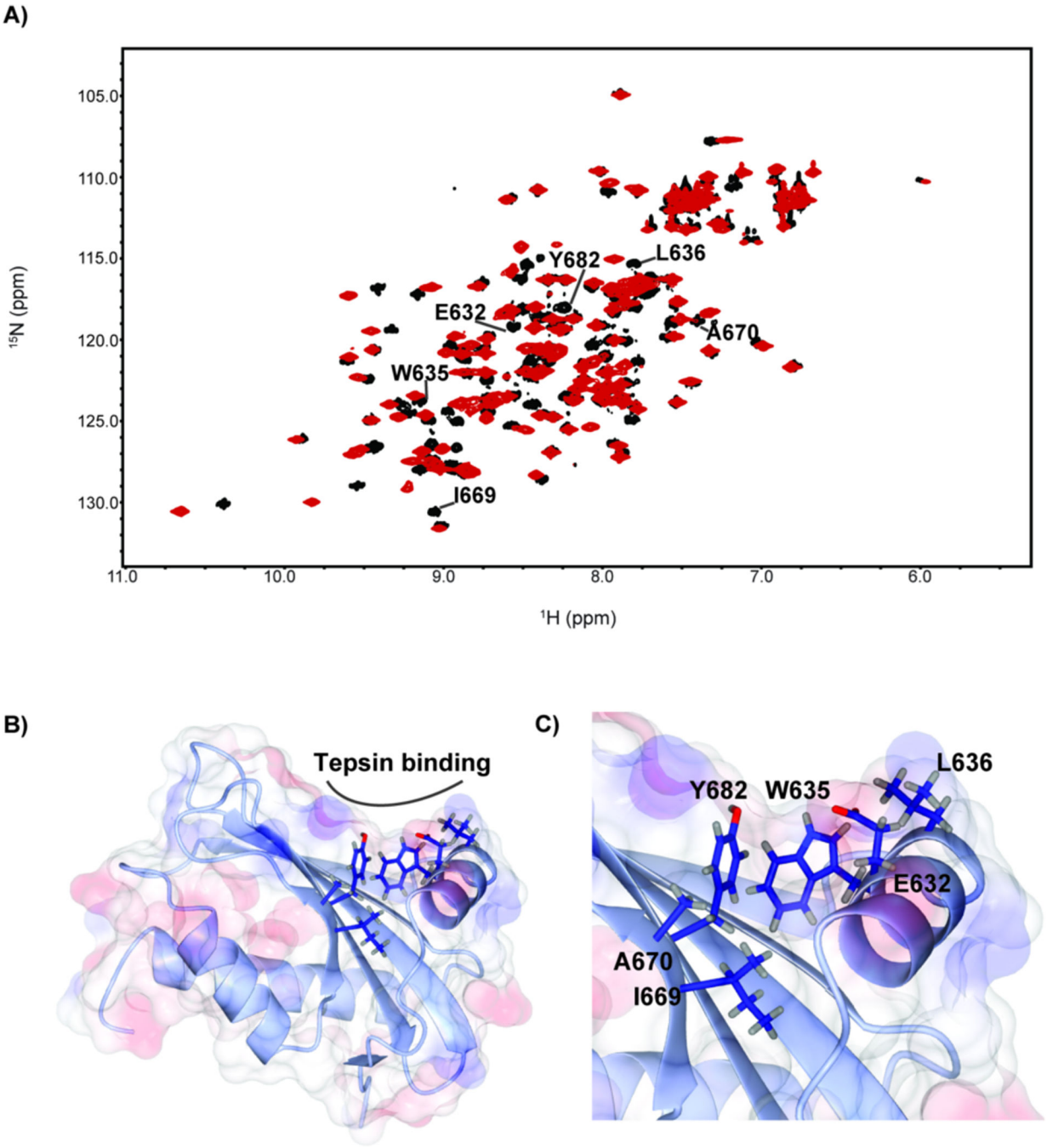

Figure 3. NMR chemical shift perturbations reveal residues on β4 surface involved in tepsin binding

A) ^{15}N-^{1}H HSQC spectra of the initial (black) and final (red) titration points show chemical shifts resulting from binding upon addition of unlabeled recombinant tepsin (residues 450–500) to labeled β4. Residues identified for further analysis are highlighted below. B) From the HSQC titration, residues that exhibited large chemical shift perturbations were mapped onto the structure (PDB 2MJ7): E632, W635, L636, I669, A670, Y682. C) Close-up view of binding interface residues identified by chemical shift perturbations.

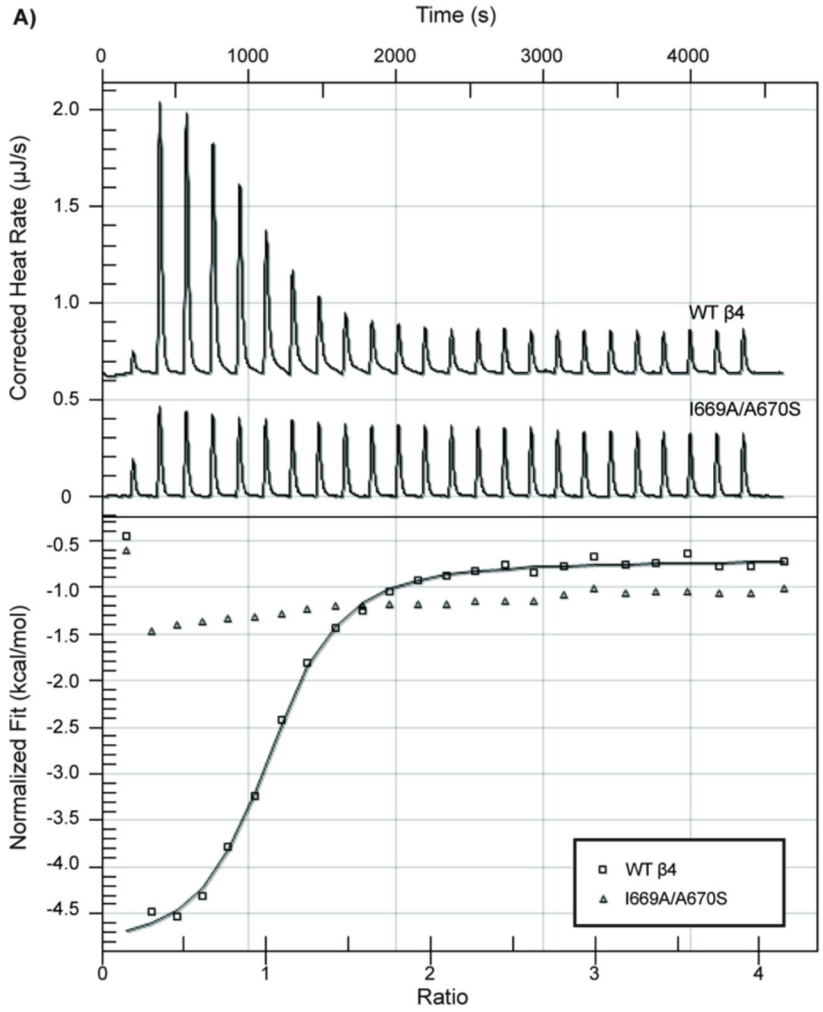

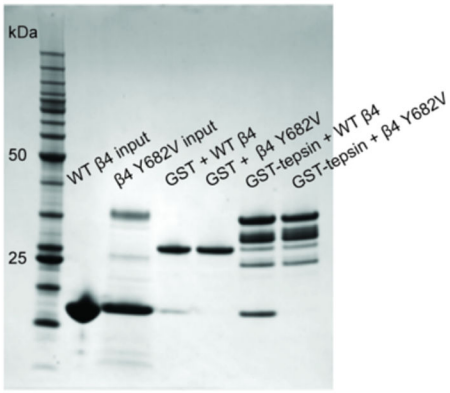

C)

β4	Tepsin	K_D (µM)
WT	WT	2.8 ± 0.8
I669A/A670S	WT	nb
Y682V	WT	nb

Figure 4. Structure-based mutagenesis of key β4 residues eliminates *in vitro* interaction with tepsin

A) The β4 mutant I669A/A670S exhibits no measurable binding to the tepsin motif by ITC (representative trace). B) Wild-type GST-tepsin (residues 450–500) pulls down wild-type β4 (positive control) but fails to pull down the β4 mutant Y682V. GST (lane 4) was used as a negative control. C) Table summarizing β4 mutant results from ITC and pulldown experiments.

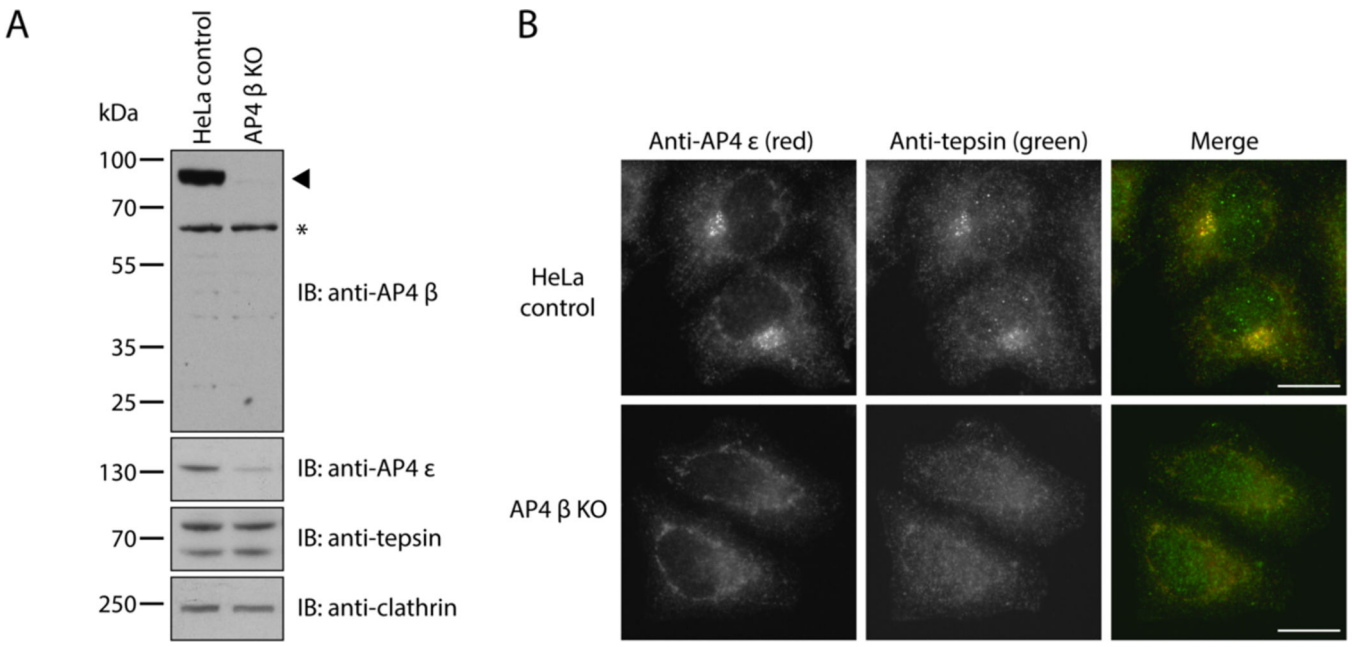

Figure 5. Tepsin is not recruited to the membrane in AP4 β4 knockout (KO) HeLa cells generated using CRISPR technology

A) Western blots of whole cell lysates from wild-type and AP4 β KO HeLa cells, probed with antibodies against AP4 β, ε, and tepsin (n.b. tepsin has two isoforms). AP4 β (marked by the arrowhead) is undetectable in the AP4 β KO cells. The band marked with the asterisk is non-specific. While the amount of AP4 ε in the AP4 β KO cells is reduced, the expression level of tepsin is unchanged. An antibody against clathrin was used as a loading control. B) Immunofluorescence double labeling for AP4 ε and tepsin in wild-type and AP4 β KO HeLa cells. In wild-type cells, tepsin labeling is punctate and concentrated in the perinuclear region where it colocalizes extensively with AP4. This pattern was absent in the AP4 β KO cells. Scale bars are 20 μm.

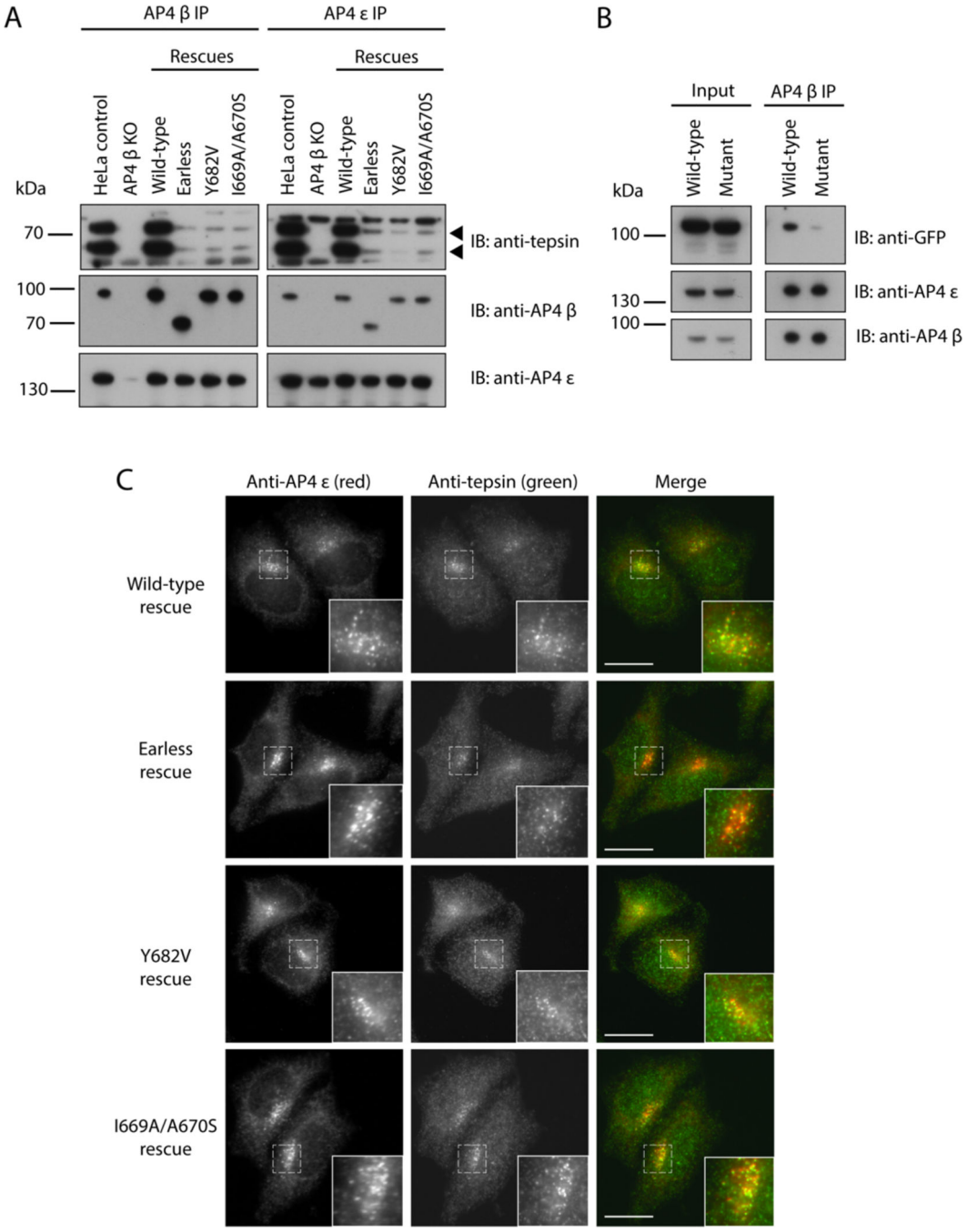

Figure 6. Disruption of the β4 appendage-tepsin interaction *in vivo* greatly reduces, but does not abolish, tepsin binding to AP4

A) Western blots of immunoprecipitates of AP4 β or ε from extracts of control (wild-type HeLa), AP4 β KO, or AP4 β KO cells stably rescued with full-length wild-type or mutant (earless, Y682V, or I669A/A670S) β4, probed with antibodies against AP4 β, ε, and tepsin (marked by arrow heads). No tepsin could be detected in the immunoprecipitates from the AP4 β KO cells, but the immunoprecipitates from the KO cells rescued with wild-type β4 contained a similar amount of tepsin to immunoprecipitates from the wild-type control cells. A small amount of tepsin was detected in the immunoprecipitates from the KO cells rescued

with mutant β4. B) Western blots of immunoprecipitates of AP4 β from extracts of HeLa cells stably expressing either wild-type or mutant tepsin-GFP (L470S/F471S), probed with antibodies against GFP, AP4 β and ε. Mutant tepsin-GFP co-immunoprecipitates with AP4 less than wild-type tepsin-GFP. C) Immunofluorescence double labeling for AP4 ε and tepsin in AP4 β KO HeLa cells stably rescued with wild-type or mutant (earless, Y682V or I669A/A670S) β4. Tepsin co-localizes with AP4 in the perinuclear region in all four rescued cell lines. Scale bars are 20 μm.